Growth of Animal Cells Around Hollow Fibers: Multifiber Studies

Charles A. Sardonini and David DiBiasio
Dept. of Chemical Engineering, Worcester Polytechnic Institute, Worcester, MA 01609

Introduction

Hollow-fiber bioreactors have been the focus of numerous mathematical modeling investigations. Models have been developed using hollow-fiber cartridges: for enzymatic catalysis (Park et al., 1981; Waterland et al., 1974); for whole cell immobilization for catalysis (Kan and Shuler, 1978; Webster and Shuler, 1978, 1979, 1981); for bacterial production (Robertson and Kim, 1985); for the measurement of diffusive permeability (Dinh and Stevenson, 1982); for enhanced nutrient transport (Schonberg and Belfort, 1987); for the analysis of intra vs. extracapillary growth (Adema and Sinskey, 1987); for optimizing fiber spacing (Chresand et al., 1988); and for modeling oxygen transport (Piret and Cooney, 1990). Due to its low solubility and high consumption rate, oxygen is often implicated as the limiting substrate in these systems (Piret and Cooney, 1990; Heath and Belfort, 1987; Glacken et al., 1983; Muller-Kleiser et al., 1982a,b, 1983, 1984; King et al., 1986, 1988).

Design equations are generally formulated on the basis of a single fiber by applying material balance equations for a given substrate to regions such as the fiber lumen, fiber wall, and extracapillary space. These equations are then extrapolated from a single fiber to a fiber bundle assuming perfect fiber spacing to predict the performance of a multifiber cartridge. Such analyses are prone to error due to the nonuniform fiber spacing problem.

In a previous study (Sardonini and DiBiasio, 1992), transfected hybridoma cells were suspended in agarose within the extracapillary space (ECS) of hollow-fiber bioreactors containing a single fiber. Both cell growth and viability were examined at various stages of development using photomicroscopy. In this system, cells were found to grow in colonies within the ECS adjacent to the fiber wall. The radial growth extent of cells away from the surface of the fiber was found to be oxygen-limited. The "penetration depth" of oxygen was defined as the radial distance away from the surface of the fiber that the oxygen concentration remains above that which was sufficient to sustain cell growth. In the single-hollow-fiber bioreactors, cells present at radial distances greater than the penetration depth were found to remain viable for several days but were incapable of division. These data were consistent with the culture of cells in oxygen-limited glass tubes (Sardonini, 1990).

A simple theoretical model was developed to predict the penetration depth using oxygen as the limiting substrate. Using oxygen consumption rates and substrate diffusivities for several growth extents, the penetration depth was found to decrease with increasing cell growth in the bioreactor. This retreating oxygen penetration depth resulted in an array of colony sizes being left behind in a region of hypoxia. The resulting profiles could be described using the diffusion-based model where colonies derived from single cells were allowed to grow in the ECS. The patterns determined experimentally correlated to those developed using the model when a random distribution of cells was used as nucleation sites for individual colonies.

To extrapolate the results obtained in single-fiber experiments to multifiber systems, the growth of transfected SPt20 cells within the extracapillary space (ECS) of bioreactors containing multiple fibers was examined. Of particular interest were the effects of fiber-fiber interactions on the growth profiles resulting from closely aligned fibers. As in the previous study, a support matrix of 0.7% agarose was provided in the ECS of the multifiber experiments to provide a support matrix and to minimize the effects of convection. Experiments corresponding to the commercial fiber packing density were performed both with and without agarose.

Materials and Methods

Hollow-fiber bioreactors were fabricated by removing hollow fibers from a CELL-PHARM hollow-fiber cartridge model I-L (gift of Unisyn Technologies, formerly C. D. Medical, Inc., Miami Lakes, FL) and suspending the fibers in the center of glass tubing using silicone sealant. Two-fiber bioreactors were evaluated using a similar design as that employed for single-hollow-fiber studies. To provide optimal growth, the dual-fiber experiments were performed using a 5% oxygen source. The cell line, materials, procedures, and analytical

Correspondence concerning this article should be addressed to D. DiBiasio.
Present address of C. A. Sardonini: CytoMed, Inc., 840 Memorial Drive, Cambridge, MA 02139.

methods employed were identical to those previously described (Sardonini and DiBiasio, 1992). To provide a control, a single-hollow-fiber bioreactor, using a 20% oxygen source, was operated in a separate system concurrently with the two-fiber bioreactor. Upon sacrificing the control and two-fiber bioreactors, the agarose cell beds were removed and sliced into approximately 1.0-mm-thick wafers at various axial distances. Wafers were examined by photomicroscopy using an Olympus BH-2 microscope to characterize axial and radial cell proliferation away from the fibers.

For the multiple-hollow-fiber bioreactor studies, medium from a 250-mL spinner vessel was fed into a single line which was split using a T-fitting. Each of the two resulting lines was passed through a Masterflex peristaltic pump into the intracapillary space (ICS) of a multiple-fiber bioreactor. Flow rates were set at 2.0 mL/min for bioreactors with five and ten fibers and 6.6 mL/min for bioreactors with 47 and 69 fibers. Upon exiting the bioreactor, the two lines were combined using a T-fitting and returned to the 250-mL spinner reservoir. In this system, medium oxygenation and pH equilibration were achieved in the medium reservoir by pumping the equilibration gas (20% oxygen, 8% CO_2, and 72% nitrogen) directly into the headspace of the spinner vessel through sterile filters. The duration of all multifiber experiments was 14 days. Experiments were performed which investigated different fiber packing densities in agarose (5, 10, 47 and 69 fibers per bioreactor) as well as a comparison with and without agarose at a packing density of 69 fibers per bioreactor. The value of 69 fibers per bioreactor corresponds to the packing density of the C.D. Medical CELL-PHARM Model I-L hollow-fiber bioreactor sold commercially.

The total cell density of multifiber bioreactors was determined by sacrificing the reactors and placing the contents (complete with fibers) into a 5.0 mL of a solution of 0.1-M citric acid, and 0.1% crystal violet. After vigorous agitation and overnight incubation at 37°C, a minimum of four samples were removed for hemacytometer nuclei counting. The total cell number within the bioreactor was determined using the calculated cell concentration along with the volume of solution.

Experimental Results

Typical experimental results for the growth of transfected cells in 0.7% agarose within the ECS of a two-fiber bioreactor are shown in Figures 1 and 2 for an equilibrated medium concentration of 5% oxygen. In the two-fiber reactor, symmetric growth patterns were observed around the fibers with large colonies located near the surface of the fiber. Smaller colonies were observed at larger radial distances, and single cells were found far from the fiber. The control culture exhibited a similar profile which was typical of operation with a 20% oxygen concentration (Sardonini and DiBiasio, 1992). Wafers for both systems examined at several axial distances along the bioreactor exhibited similar penetration profiles away from the fiber suggesting the absence of axial oxygen gradients. Since the fibers were not perfectly straight, the area of intersecting growth space between the two fibers varied with axial position. Figure 1 demonstrates a case where the two fibers were at such a distance apart that the cell growth areas did not overlap. Here it can be seen that the profiles observed from each of the two fibers within the same bioreactor were nearly identical.

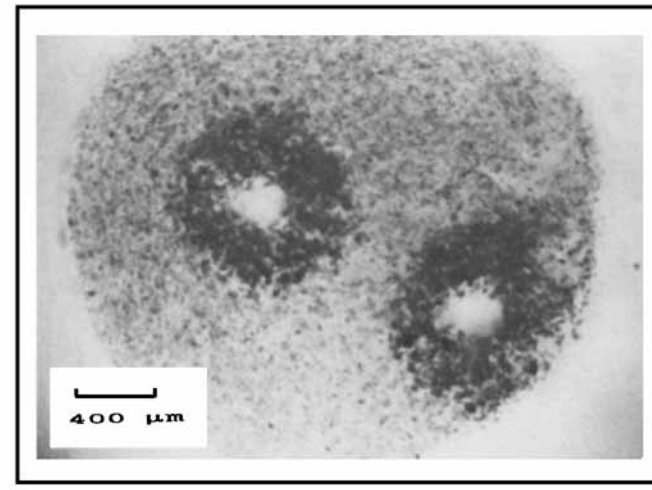

Figure 1. Typical experimental results for the growth of SPt20 cells in two-fiber bioreactors in areas where the fiber profiles did not interact.

Figure 2 exhibits an example of cell growth areas between two fibers which interact with each other as well as with the wall of the bioreactor. The profiles demonstrated by the two intersecting growth areas overlapped in such a manner that the presence of one fiber had an undetectable effect on the growth profile of the opposite fiber. In other words, the interaction between the growth areas of the fibers resulted in no observable increase or decrease in cell growth other than simple overlap of profiles. Figure 2 also shows that the distortion effect of the bioreactor wall on the cell growth profile was minimal.

For reactors with more than two fibers, wafers could not be removed and examined by photomicroscopy as in the one- and two-fiber experiments. Evidence of cell growth could only be qualitatively assessed through visual observation of the exterior of the reactors. From these visual observations, it was noted that growth in the multifiber reactors differed from

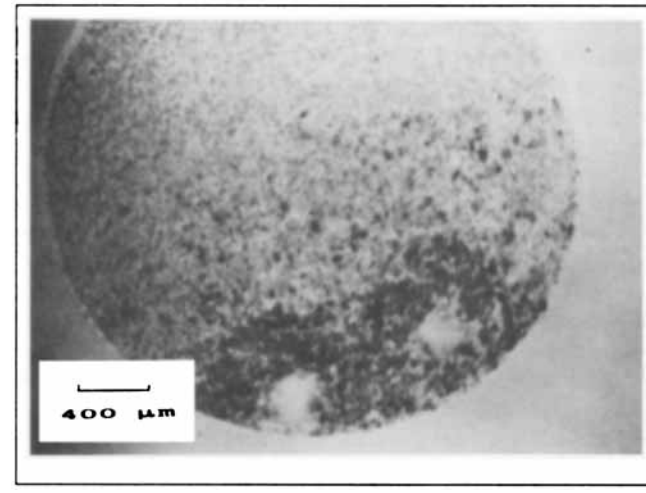

Figure 2. Typical experimental results for the growth of SPt20 cells in two-fiber bioreactors in areas where fiber-fiber and fiber-wall interactions were present.

Table 1. Experimental and Theoretical Cell Concentrations for Operation of Multihollow-Fiber Bioreactors at Different Fiber Densities*

No. of Fibers per bioreactor	5	10	47	69
Fiber Density (Fibers/cm^2)	71	140	660	980
Cell Density (with Agarose)	2.5×10^7	5.0×10^7	1.9×10^7	2.2×10^7
				4.3×10^7
Cell Density (No Agarose)	-	-	-	3.2×10^7
Predicted Cell Density	2.7×10^7	5.4×10^7	$16.\times10^7$	$15.\times10^7$

*Cell densities represent cells per milliliter of bioreactor volume (ECS + ICS + fiber wall volume).

previous experimental results with one- and two-fiber experiments in that the growth patterns were not uniform. The one- and two-fiber experiments demonstrated a uniform cell mass surrounding the wall of each fiber. In the multifiber experiments, cells could be seen to form regions of high density adjacent to some fibers while maintaining regions of low density adjacent to other fibers. These nonuniformities were observed both in the axial and radial directions.

At the termination of the multifiber experiments, the cell densities within the bioreactors were enumerated using the nuclei-counting methodology previously described. The cell densities observed in bioreactors containing different fiber concentrations are given in Table 1. Cell densities are expressed as total cells per mL of bioreactor volume (ECS + ICS + fiber wall volume). In each of these experiments, the cell growth within the bioreactor was nonuniform exhibiting areas of high cell densities as well as void spaces displaying little cell growth. The highest cell density of 5.0×10^7 total cells/mL bioreactor was obtained in an experiment using ten fibers.

Model Development

To provide a quantitative basis for the prediction of cell growth in commercial hollow-fiber units, a simplified model of these idealized reactors was developed (Sardonini and DiBiasio, 1992), using oxygen as the limiting substrate. When analyzing the growth of cells around single-hollow fibers, the analysis was based on each cell acting as a nucleation point for an individual colony. As colonies grew in size, substrate gradients were realized both within individual colonies as well as away from individual fibers. Further cell growth results in regions of oxygen depletion within the ECS. The radius at which oxygen concentrations fall below those necessary to support cell growth was termed the "penetration depth." Rather than solve the full set of dynamic equations describing this process, the model approximates the system by using colony size as an indirect measure of time. The model accounts for oxygen consumption within each colony and the variability in the oxygen diffusivity with increasing cell mass.

Visual inspection of commercial hollow-fiber bioreactors indicates that fiber spacing is not uniform. The distance between any two fibers varies with position in the bioreactor. Mathematical models based on single-fiber material balance equations that assume perfect fiber spacing are subject to error due to the problem of overlapping cell growth areas due to the presence of nonuniform spacing. The amount of error depends on the degree of nonuniformity of fiber spacing. This degree of nonuniformity can be described by two limiting cases in Figure 3. Figure 3a demonstrates the case of perfect fiber

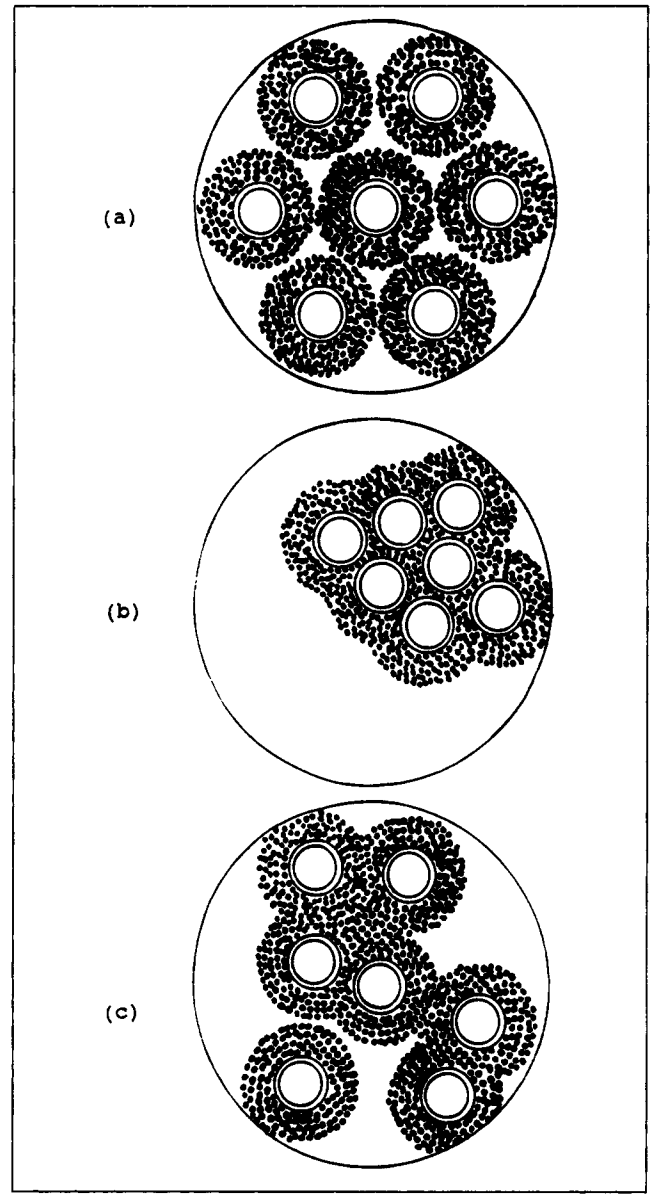

Figure 3. Cross-sectional area showing (a) perfect fiber spacing, (b) bunched fiber spacing, and (c) random fiber spacing.

spacing. Here, little or no overlap of cell growth area will be observed in the reactor (depending on the operational conditions). In this scenario, mathematical models based on perfect fiber spacing will have minimal error due to the overlapping growth area problem. The second limiting case in Figure 3b is when all the fibers are bunched into a small area within the reactor (fibers close together with respect to cell penetration depths). In this case, overlapping cell growth areas can be significant resulting in large errors in the perfect fiber spacing models. A situation between the "perfect" and "bunched" cases is the case of random fiber spacing in Figure 3c. For this situation, the problem of overlapping cell growth areas may not be minimized although it is not as severe as is the case with "bunched" fibers. As a compromise between the cases of "perfect" and "bunched" fiber spacing, the case of random

fiber spacing was investigated to simulate the fiber spacing theoretically in commercial hollow-fiber cartridges.

To determine the volume of viable cells in a bioreactor with randomly spaced fibers, the cross-sectional area profiles of randomly spaced fibers were generated by computer using a random number generator to place fibers in the ECS of a hollow-fiber bioreactor. This was accomplished by generating points on an x,y plane which were used as the centers of circles which represent the fiber outer diameter. Care was taken to insure that the fiber circles would not overlap as this would be an unrealistic condition. It is possible to calculate analytically the area occupied by viable cells in diagrams such as Figure 3c. However, the calculation becomes difficult when more than three cell growth extents overlap and is particularly tedious for fiber placements such as Figure 3b. Thus, a numerical approach was used to make the calculation. Using the generated fiber location diagrams, the volumes in the bioreactor filled with viable cells were calculated using the following methodology:

1. Cross-sectional profiles for bioreactors with different fiber densities were generated by distributing the fibers with a random number generator as previously described.
2. Using the single-fiber model, the penetration depth of viable cells away from each fiber was determined (assuming a continuous cell mass was present) using Eq. 11 (Saronini and DiBiasio, 1992).
3. Using the random number generator, 5,000 test points were distributed randomly in the bioreactor. Each test point was monitored to determine if it was placed inside a fiber, within the cell mass, or within an area void of viable cells (outside of the cell penetration depth of all fibers). A statistical and numerical analysis showed that 5,000 points were more than sufficient to generate accurate area determinations.
4. The percent growth area in the profile was determined by dividing the number of test points in the viable cell mass by the total number of test points attempted.
5. The area determined in step 4 was multiplied by the reactor length.

Since the crystal violet/citric acid procedure used to experimentally determine the cell density within the bioreactors measures both viable and nonviable cells, it was necessary to modify the procedure previously described to include the cells in the oxygenated regions adjacent to the fiber walls (presumably viable) as well as the cells in the hypoxic regions away from the fibers (presumably nonviable) into a total cell count. This would allow a more accurate comparison of the results determined theoretically from the results obtained by experiment. To provide a basis for the total cell count, the total cell density at different time intervals after seeding was determined. This was accomplished by starting with an initial seeding concentration and by incrementing the colony sizes and penetration depths according to the scheme used for the model development in the single-fiber bioreactors as previously mentioned. This simplified model essentially used colony size as an indirect measure of time. Using this technique, the area corresponding to different cell density ranges could be determined for several time periods post inoculation. This allowed an approximation of the cell density within the region of hypoxia in the extracapillary space. Total cell counts were determined by adding the viable cell population in the oxygenated areas to the nonviable population in the hypoxic regions for each corresponding penetration depth. Results simulating the conditions of the experiments reported here are presented in Table 1.

Discussion

The experimental results for the two-fiber reactors were similar to those of the single-hollow-fiber experiments for a 5% oxygen concentration (Sardonini and DiBiasio, 1992) with regard to cell growth profiles around the fibers. This indicates that the substrate transport and consumption processes which yielded the growth profile for one fiber are governing each of the two fibers in the two-fiber experiment. No difference in profiles in the axial direction were observed with regard to cell growth around either of the two fibers. This indicates that the partitioning of medium flow between the two fibers was even enough to keep the oxygen concentration at the surface of both fibers uniform. Similar profiles between the fibers placed far apart shown in Figure 1 suggest that the fibers are acting identically. The absence of interaction between the two fibers indicates that when the fibers are far enough apart such that their cell growth profiles do not interact, the system can be described by doubling the single-hollow-fiber results.

For the case of fiber-fiber overlap, the resulting cell growth profiles observed do not show any signs of deformation due to the overlapping phenomenon. This result is expected due to the absence of an oxygen gradient at the midpoint between hollow fibers. This infers that there is no transport of oxygen between the cell growth areas supported by different fibers in this system.

A comparison of theoretical and experimental results for multifiber operation is shown in Table 1. While the results at low fiber densities show good agreement between theory and experiment, modeling results at high fiber densities significantly overpredict cell concentrations when compared to experimental values. Note that the predicted cell density decreases at the highest fiber density. This is due to the fact that at 980 fibers/cm^2, the system becomes overpacked with fibers. The available volume for cell growth is less than optimal.

There are several possible reasons for the overprediction of cell concentration at high fiber densities. Every multihollow fiber run with greater than two fibers per bioreactor displayed some nonuniform cell growth. Some areas within the bioreactors were densely packed with cells, while other areas showed little cell growth. Possible explanations include: the use of agarose in the experiments, maldistribution of flow to the lumen of the reactors, and nonuniform inoculation of cells. The model does not account for any of these effects. The experimental results at 69 fibers per reactor showed very similar cell densities with and without agarose. This suggests that the difference between model and experiment is not due to the use of agarose. If some tubes of a multifiber reactor were fed at different feed flows than others, nonuniform cell growth patterns may result. However, since the same feed distribution setup was used in all multifiber runs, one would have expected to observe this effect to some degree in all experiments. This was not the case. It seems most likely then that nonuniform inoculation of cells to the reactors with high fiber densities would be the major reason for model overpredictions. This effect would be more pronounced when more fibers were present, making it more difficult for the inoculum to distribute

equally throughout the ECS. The model would have to be modified to include an inoculum effect to verify this.

It is interesting to note that a significant overprediction of cell densities was also observed by Chresand et al. (1988) using an oxygen-limited, diffusion-controlled model to predict the growth of EAT cells around Celgard X-20 hollow fibers. These authors suggested that toxic effects from lactate buildup may have contributed to decreased cell densities.

Acknowledgment

The authors would like to thank Richard Schoenfeld, Debra Barngrover, and Genzyme Corporation for financial and technical support and Robert A. Kennerly for photographic assistance.

Literature Cited

Adema, E., and A. J. Sinskey, "An Analysis of Intra-Versus Extracapillary Growth in a Hollow Fiber Reactor," *Biotechnol. Prog.*, 3(2), 74 (1987).

Chresand, R. T., B. E. Dale, and R. J. Gillies, "Optimum Fiber Spacing in a Hollow Fiber Bioreactor," *Biotechnol. Bioeng.*, **32**(8), 983 (1988).

Dinh, S. M., and J. F. Stevenson, "A Transient Experiment to Measure the Diffusive Permeability of Hollow Fiber Membranes," *J. Membr. Sci.*, **11**, 127 (1982).

Glacken, M. W., R. J. Fleischaker, and A. J. Sinskey, "Large-Scale Production of Mammalian Cells and Their Products: Engineering Principles and Barriers to Scale Up," *Anal. N.Y. Acad. Sci.*, **413**, 355 (1983).

Heath, C., and G. Belfort, "Immobilization of Suspended Mammalian Cells: Analysis of Hollow Fiber and Microcapsule Bioreactors," *Advances in Biochemical Engineering/Biotechnology*, A. Fiechter, ed., Springer-Verlag, p. 1 (1987).

Kan, J. K., and M. L. Shuler, "Urocanic Acid Production Using Whole Cells Immobilized in a Hollow Fiber Reactor," *Biotechnol. Bioeng.*, **20**, 217 (1978).

King, W. E., D. S. Schultz, and R. A. Gatenby, "Multiregion Models for Describing Oxygen Tension Profiles in Human Tumors," *Chem. Eng. Commun.*, **47**, 73 (1986).

King, W. E., D. S. Schultz, and R. A. Gatenby, "An Analysis of Systemic Tumor Oxygenation Using Multiregion Models," *Chem. Eng. Commun.*, **64**, 137 (1988).

Muller-Kleiser, W., "Method for the Determination of Oxygen Consumption Rates and Diffusion Coefficients in Multicellular Spheroids," *Biophys. J.*, **46**, 343 (1984).

Muller-Kleiser, W., and R. M. Sutherland, "Influence of Convection in the Growth Medium on Oxygen Tensions in Multicellular Spheroids," *Cancer Res.*, **42**, 237 (1982a).

Muller-Kleiser, W., and R. M. Sutherland, "Oxygen Tensions of Multicell Spheroids of Two Cell Lines," *Brit. J. Cancer*, **45**, 256 (1982b).

Muller-Kleiser, W., and R. M. Sutherland, "Frequency Distribution Histograms of Oxygen Tensions in Multicell Spheroids," *Adv. Expt. Med. Biol.*, **159**, 497 (1983).

Park, T. H., I. H. Kim, and H. N. Chang, "Recycle Hollow Fiber Enzyme Reactor with Flow Swing," *Biotechnol. Bioeng.*, **27**, 1185 (1981).

Piret, J. M., and C. L. Cooney, "Mammalian and Cell Protein Distributions in Ultrafiltration Hollow Fiber Bioreactors," *Biotechnol. Bioeng.*, **36**, 902 (1990).

Robertson, C. R., and I. H. Kim, "Dual Aerobic Hollow-Fiber Bioreactor for Cultivation of *Streptomyces Aureofaciens*," *Biotechnol. Bioeng.*, **27**, 1012 (1985).

Sardonini, C. A., and D. DiBiasio, "An Investigation of the Diffusion Limited Growth of Animal Cells Around Single Hollow Fibers," *Biotechnol. Bioeng.*, **40**, 1233 (1992).

Sardonini, C. A., "An Investigation into the Growth of Animal Cells around Single and Multiple Hollow Fibers," PhD Thesis, Worcester Polytechnic Institute, Worcester, MA (1990).

Schonberg, J. A., and G. Belfort, "Enhanced Nutrient Transport in Hollow Fiber Perfusion Bioreactors: a Theoretical Analysis," *Biotechnol. Prog.*, **3**(2), 80 (1987).

Waterland, L. R., A. S. Michaels, and C. R. Robertson, "A Theoretical Model for Enzymatic Catalysis Using Asymmetric Hollow Fiber Membranes," *AIChE J.*, **20**(11), 50 (1974).

Webster, I. A., and M. L. Shuler, "Mathematical Models for Hollow Fiber Enzyme Reactors," *Biotechnol. Bioeng.*, **20**, 1541 (1978).

Webster, I. A., and M. L. Shuler, "The Measurement of Effective Substrate Diffusivities within Whole Cell Suspensions Using a Diffusion-Limited Hollow Fiber Reactor," *J. Chem. Tech. Biotechnol.*, **31**, 226 (1981).

Webster, I. A., M. L. Shuler, and P. R. Rony, "Whole-Cell Hollow Fiber Reactor: Effectiveness Factors," *Biotechnol. Bioeng.*, **21**, 1725 (1979).

Manuscript received June 29, 1992, and revision received Jan. 28, 1993.